# Supplementary Information

**Redox Potential Regulation Toward Suppressing Hydrogen Evolution in Aqueous Sodium-ion Batteries: $Na_{1.5}Ti_{1.5}Fe_{0.5}(PO_4)_3$**

Yuegang Qiu, Yonghui Yu, Jia Xu, Yi Liu, Mingyang Ou, Shixiong Sun, Peng Wei, Zhi Deng, Yue Xu, Chun Fang, Qing Li, Jiantao Han*, and Yunhui Huang

State Key Laboratory of Material Processing and Die &Mould Technology

School of Materials Science and Engineering

Huazhong University of Science and Technology

Wuhan 430074, P. R. China

**Corresponding Author**

*E-mail: jthan@hust.edu.cn (Prof. Jiantao Han)

**Table S1.** Lattice parameters of $NaTi_2(PO_4)_3$ (NTP) and $Na_{1.5}Ti_{1.5}Fe_{0.5}(PO_4)_3$ (NTFP).

| | a(Å) | b(Å) | c(Å) | Volume(Å$^3$) | α | β | γ |
|---|---|---|---|---|---|---|---|
| NTP | 8.513 | 8.513 | 21.692 | 1361.455 | 90 | 90 | 120 |
| NTFP | 8.532 | 8.532 | 21.775 | 1372.743 | 90 | 90 | 120 |

**Table S2.** Structure parameters of $NaTi_2(PO_4)_3$ (NTP) and $Na_{1.5}Ti_{1.5}Fe_{0.5}(PO_4)_3$ (NTFP) obtained from Rietveld refinement.

| NTP | | | | NTFP | | | |
|---|---|---|---|---|---|---|---|
| Name | Fractional coordinates | Mult | Occupancy | Name | Fractional coordinates | Mult | Occupancy |
| O1 | 0.1736, -0.0285, 0.1930 | 36 | 1 | O1 | 0.1736, -0.0285, 0.1930 | 36 | 1 |
| O2 | 0.1955, 0.1648, 0.085 | 36 | 1 | O2 | 0.1955, 0.1648, 0.085 | 36 | 1 |
| Na1 | 0, 0, 0 | 6 | 1 | Na1 | 0, 0, 0 | 6 | 1 |
| Ti1 | 0, 0, 0.1455 | 12 | 1 | Na2 | 0.6424, 0, 0.2500 | 18 | 0.1667 |
| P1 | 0.2879, 0, 0.2500 | 18 | 1 | Ti1 | 0, 0, 0.1455 | 12 | 0.7519 |
| | | | | Fe1 | 0, 0, 0.1455 | 12 | 0.2481 |
| | | | | P1 | 0.2879, 0, 0.2500 | 18 | 1 |

**Table S3.** Bond values of $NaTi_2(PO_4)_3$ (NTP) and $Na_{1.5}Ti_{1.5}Fe_{0.5}(PO_4)_3$ (NTFP) obtained from Rietveld refinement.

| | Length (Å) | Angle (°) | | |
|---|---|---|---|---|
| | Ti1(Fe1)-O1 | Ti1-O1-P1 | O1-P1-O2 | O1-Ti1-O2 |
| NTP | 1.914 | 153.286 | 111.602 | 89.842 |
| NTFP | 1.919 | 153.291 | 111.566 | 89.904 |

**Table S4.** XPS quantification report of $NaTi_2(PO_4)_3$ (NTP) and $Na_{1.5}Ti_{1.5}Fe_{0.5}(PO_4)_3$ (NTFP).

| Sample | Peak | Position BE (eV) | Atomic mass | Atomic Conc % | Mass Conc % |
|---|---|---|---|---|---|
| NTP | Na 1s | 1068.00 | 22.990 | 0.94 | 1.27 |
| | O 1s | 528.60 | 15.999 | 40.15 | 37.63 |
| | Ti 2p | 457.35 | 47.878 | 4.02 | 11.27 |
| | P 2p | 131.15 | 30.974 | 10.10 | 18.32 |
| | C 1s | 282.25 | 12.011 | 44.79 | 31.51 |
| NTFP | Na 1s | 1067.70 | 22.990 | 0.96 | 1.29 |
| | O 1s | 527.90 | 15.999 | 41.97 | 39.17 |
| | Ti 2p | 456.75 | 55.846 | 3.17 | 8.85 |
| | Fe 2p | 709.55 | 47.878 | 0.61 | 2.00 |
| | P 2p | 130.45 | 30.974 | 10.27 | 18.56 |
| | C 1s | 281.950 | 12.011 | 43.02 | 30.14 |

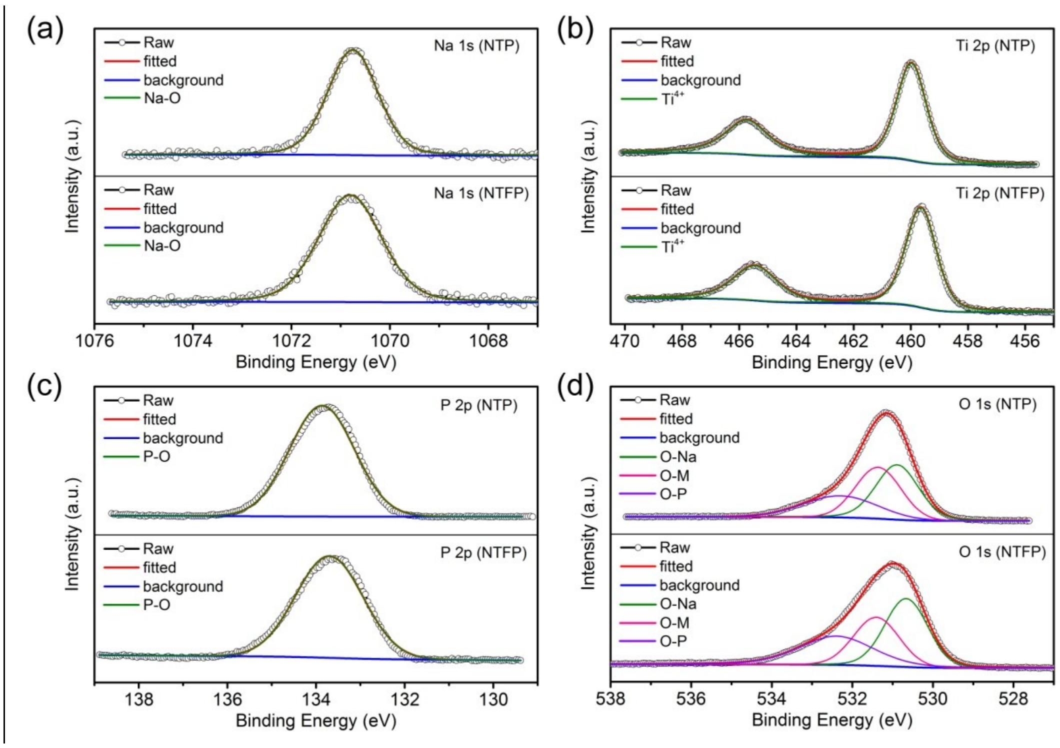


**Fig. S1.** XPS detail spectra of (a) Na 1s, (b) Ti 2p, (c) P 2p, and (d) O 1s for the $NaTi_2(PO_4)_3$ (NTP) and $Na_{1.5}Ti_{1.5}Fe_{0.5}(PO_4)_3$ (NTFP) samples.

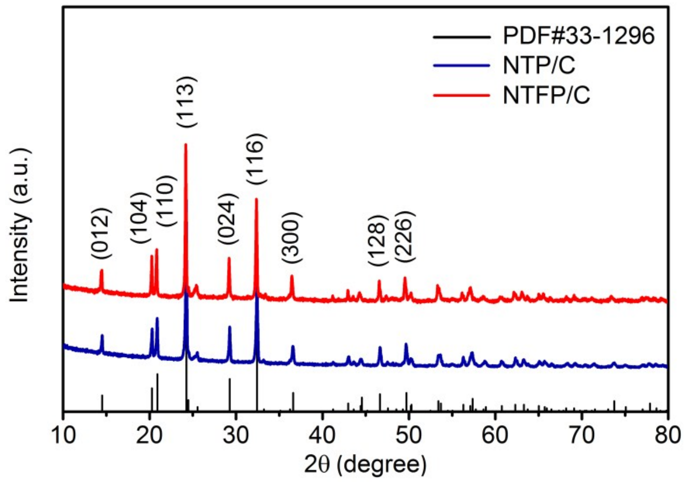


**Fig. S2.** XRD patterns of $NaTi_2(PO_4)_3/C$ (NTP/C) and $Na_{1.5}Ti_{1.5}Fe_{0.5}(PO_4)_3/C$ (NTFP/C).

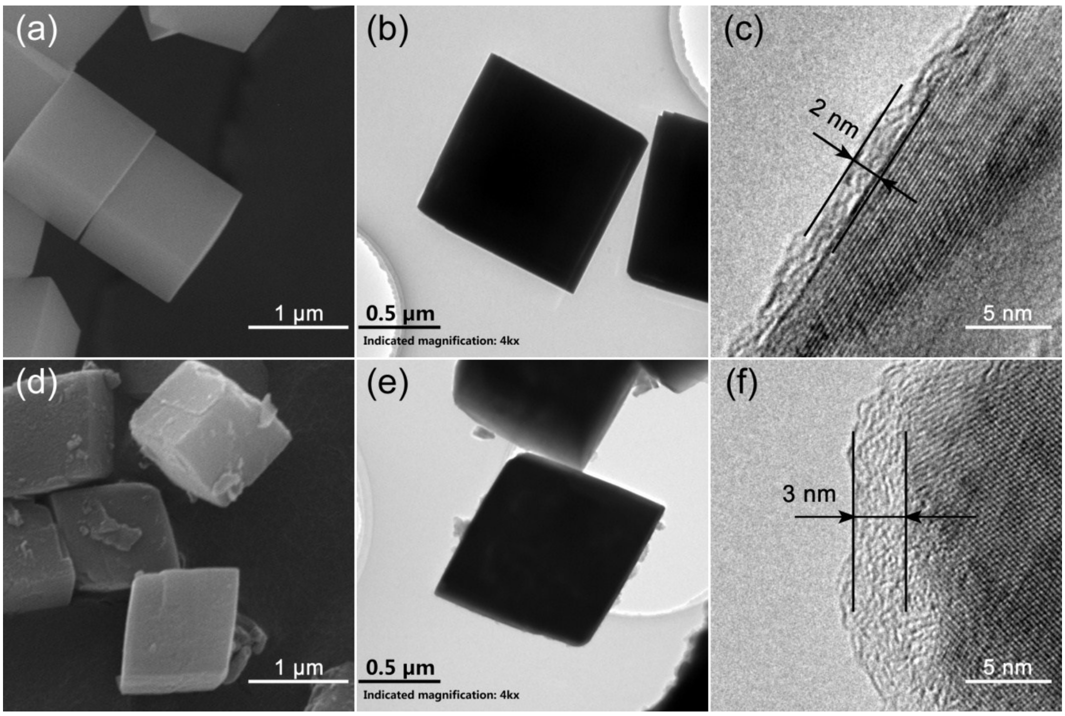


**Fig. S3.** SEM and TEM images of (a-c) $NaTi_2(PO_4)_3/C$ (NTP/C, carbon layer: 2 nm) and (d-f) $Na_{1.5}Ti_{1.5}Fe_{0.5}(PO_4)_3/C$ (NTFP/C, carbon layer: 3 nm).

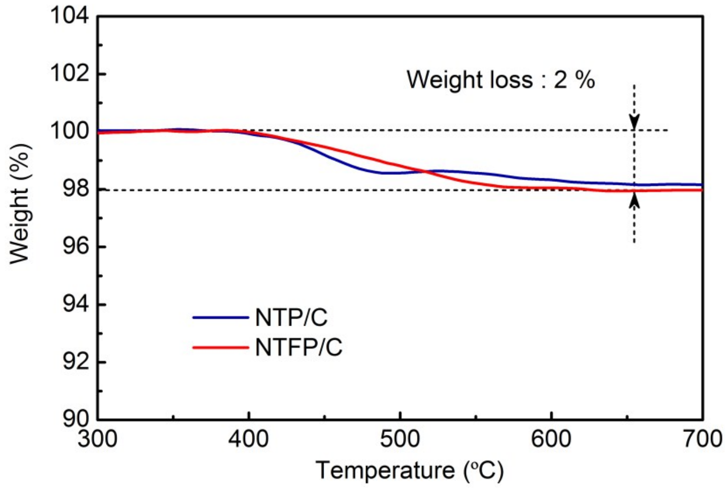


**Fig. S4.** TG curves of $NaTi_2(PO_4)_3/C$ (NTP/C) and $Na_{1.5}Ti_{1.5}Fe_{0.5}(PO_4)_3/C$ (NTFP/C).

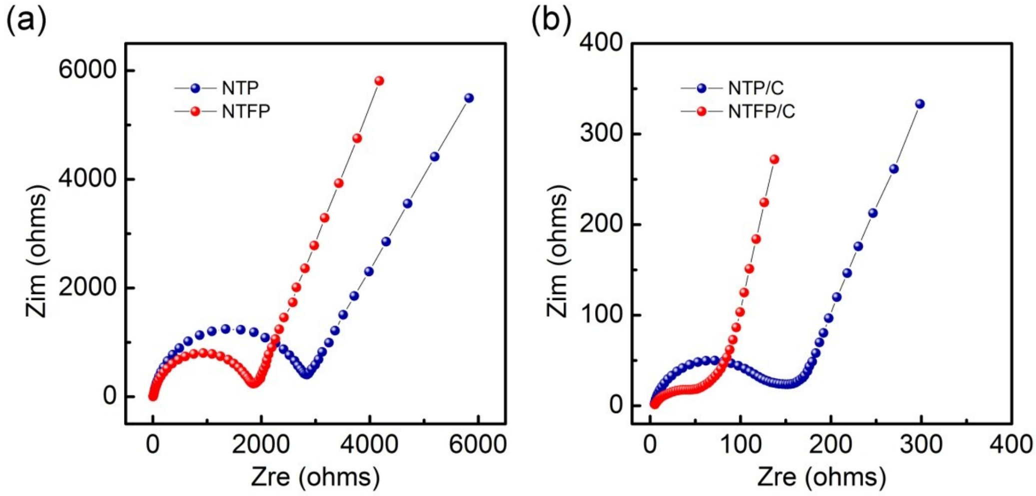


**Fig. S5.** The Nyquist plots of $NaTi_2(PO_4)_3$ (NTP) and $Na_{1.5}Ti_{1.5}Fe_{0.5}(PO_4)_3$ (NTFP) (a) before and (b) after carbon coated (fresh half cells with metallic sodium as contour electrode).

The impedances of the cells assembled by the carbon-coated samples are greatly reduced, indicating that the carbon layer greatly improves the conductivity of the samples. And, regardless of carbon coating or not, the cell impedance of the Fe-substituted sample is lower than the non-substituted one, indicating that the Fe substitution improves the conductivity of the sample.

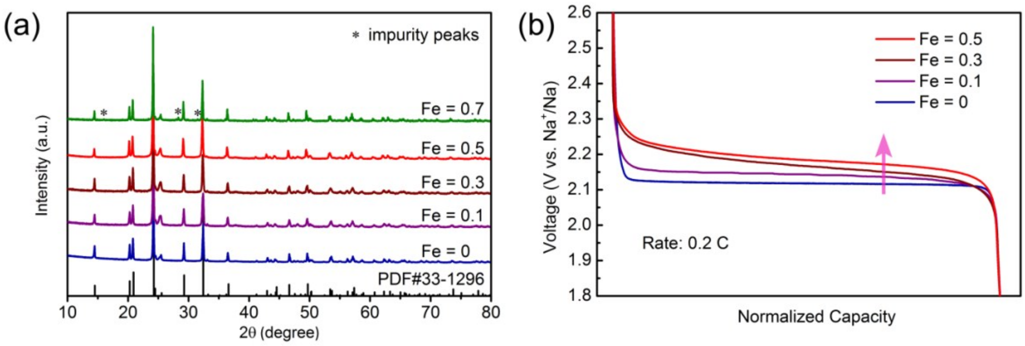


**Fig. S6. (**a) XRD patterns and (b) discharge curves of samples with different Fe substituted content $Na_{1+x}Ti_{2-x}Fe_x(PO_4)_3/C$.

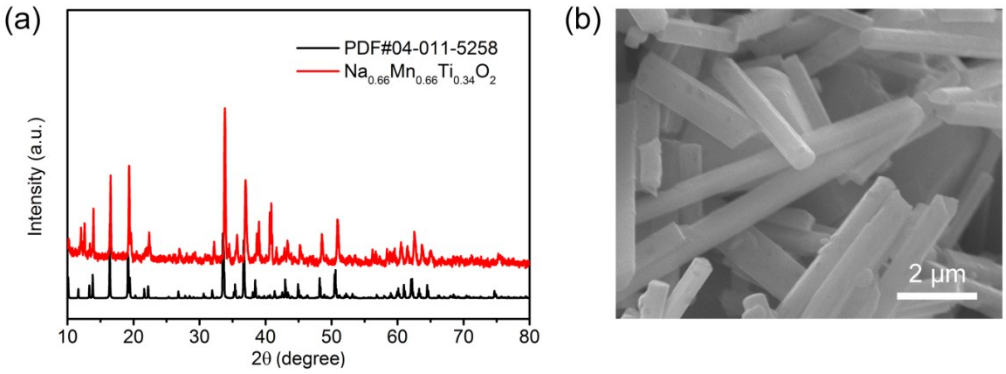


**Fig. S7.** (a) XRD pattern and (b) morphology of $Na_{0.66}Mn_{0.66}Ti_{0.34}O_2$

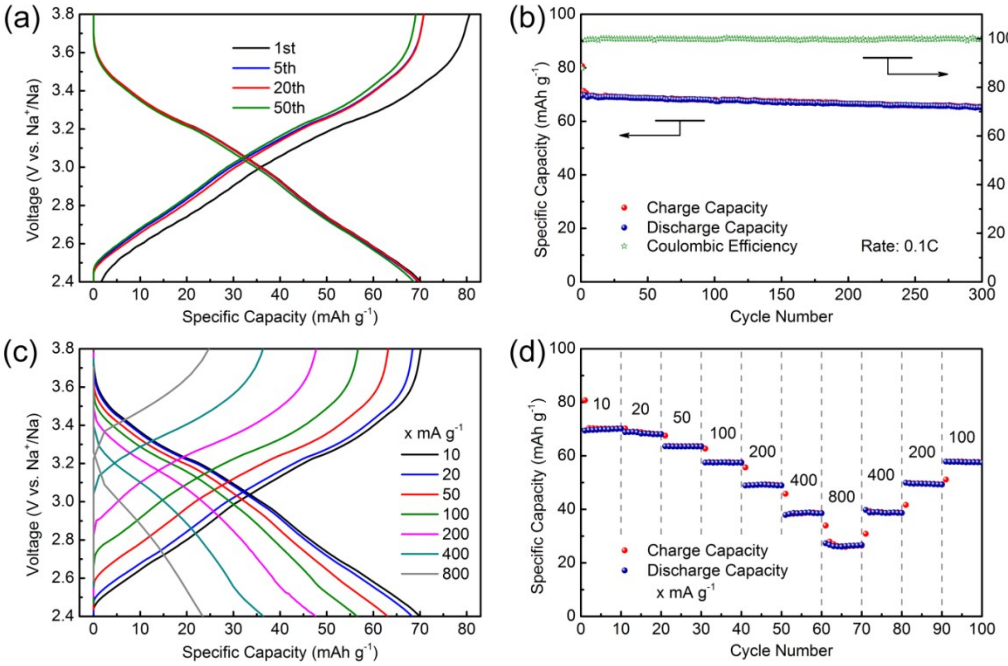


**Fig. S8.** Sodium storage performances of $Na_{0.66}Mn_{0.66}Ti_{0.34}O_2$ (NMTO) in the non-aqueous electrolyte. (a) Charge-discharge curves at 0.1C rate. (b) Long-cycle performance at 0.1C rate. (c) Charge-discharge curves at different rates. (d) Cycle performance of at different rates.

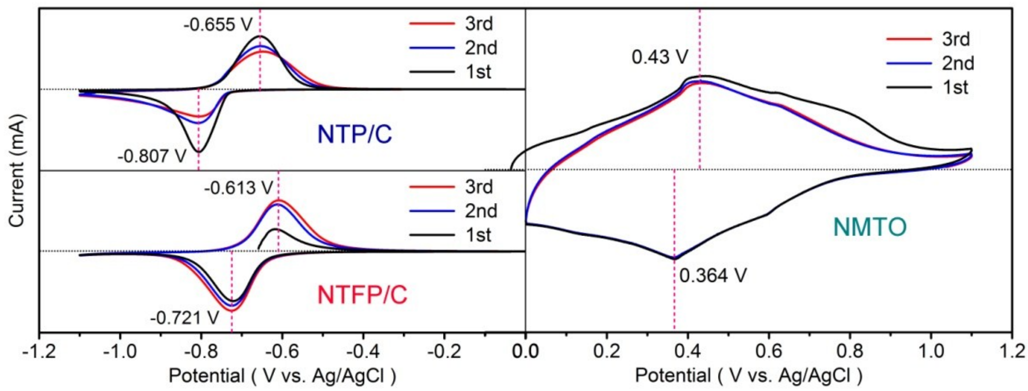


**Fig. S9.** The first three CV curves of $Na_{0.66}Mn_{0.66}Ti_{0.34}O_2$ (NMTO), $NaTi_2(PO_4)_3$ /C (NTP/C) and $Na_{1.5}Ti_{1.5}Fe_{0.5}(PO_4)_3$ /C(NTFP/C) in the aqueous electrolyte at a scan rate of 1 mV $s^{-1}$.

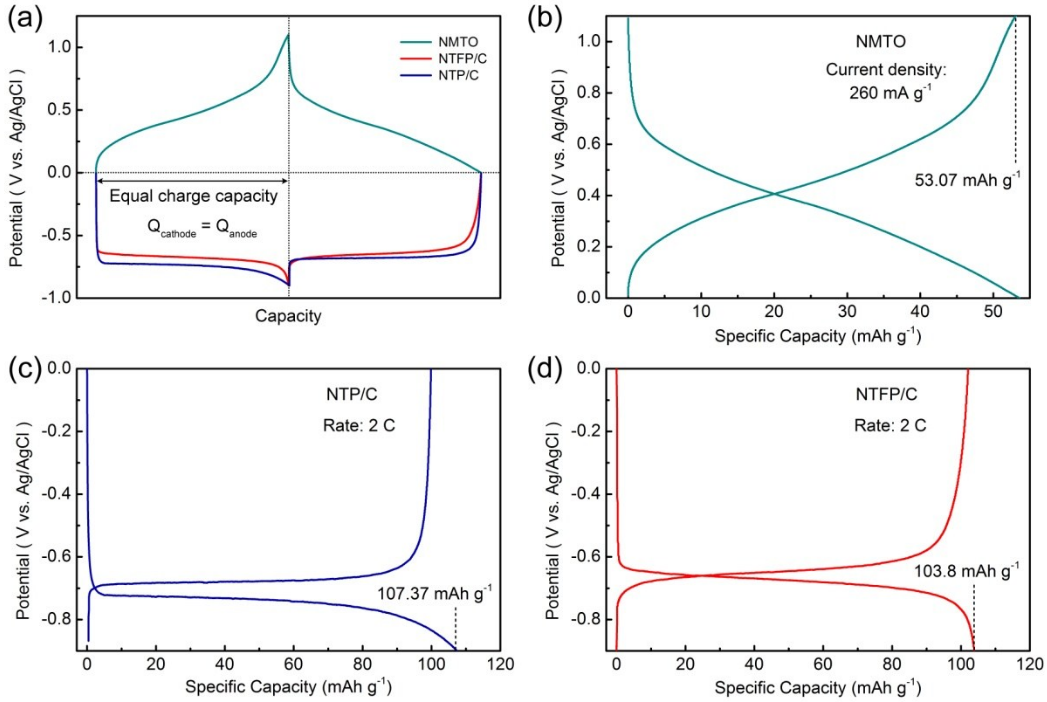


**Fig. S10.** (a) Matchup parameters of the aqueous full cell (Charge capacity: $Q_{cathode}$ = $Q_{anode}$.). Charge-discharge curves of (b) $Na_{0.66}Mn_{0.66}Ti_{0.34}O_2$ (NMTO), (c) $NaTi_2(PO_4)_3$/C (NTP/C), and (d) $Na_{1.5}Ti_{1.5}Fe_{0.5}(PO_4)_3$/C (NTFP/C) half cells in the aqueous electrolyte at a same current density.

For NMTO-NTP/C aqueous full cell, mass(NMTO)*53.07 = mass(NTP/C)*107.37, and for NMTO-NTFP/C is mass(NMTO)*53.07 = mass(NTP/C)*103.8

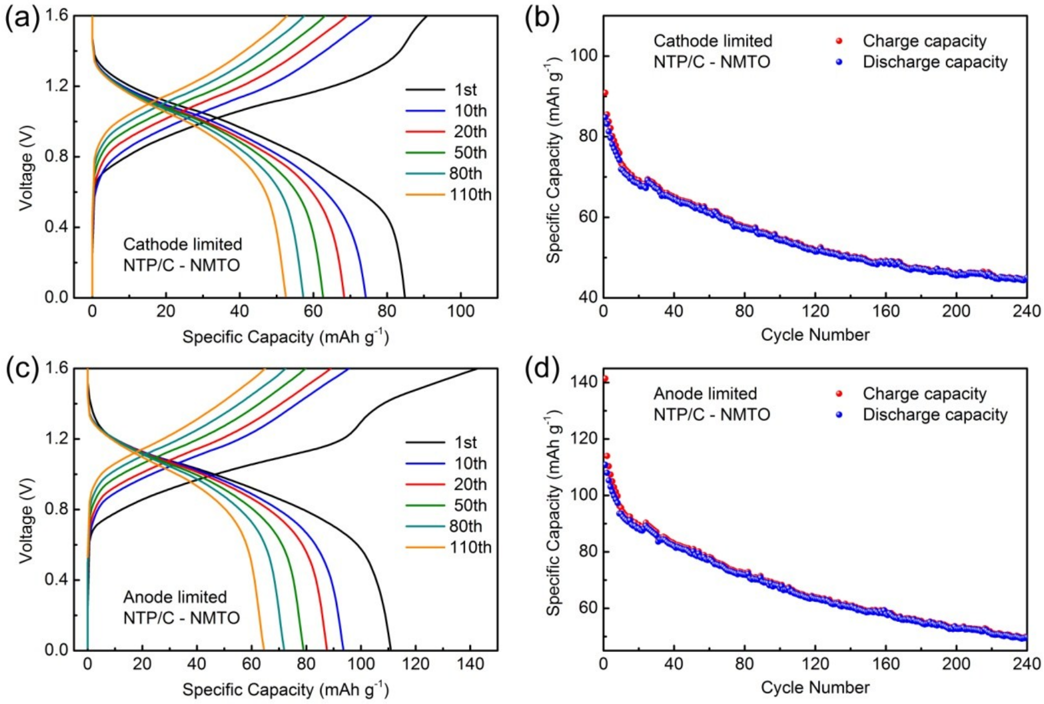


**Fig. S11.** (a, c) Charge-discharge curves and (b, d) cycle performance of the (a, b) Cathode and (c, d) anode limited style $Na_{0.66}Mn_{0.66}Ti_{0.34}O_2$-$NaTi_2(PO_4)_3$/C (NMTO-NTP/C) aqueous full cells at 2 C rate.

Cathode limited means the anode is 10% extra than the cathode, and anode limited means the cathode is 10% than the anode.

For $Na_{0.66}Mn_{0.66}Ti_{0.34}O_2$-$NaTi_2(PO_4)_3$/C (NMTO-NTP/C) aqueous full cell, when it is cathode limited, the excessive anode will slightly restrain the hydrogen evolution in the charging process, while when it is anode limited, the hydrogen evolution will be aggravated. However, due to the low operating potential of NTP/C, hydrogen evolution is inevitable in both forms of the aqueous full cells, leading to a sharp deterioration of cycle performance.

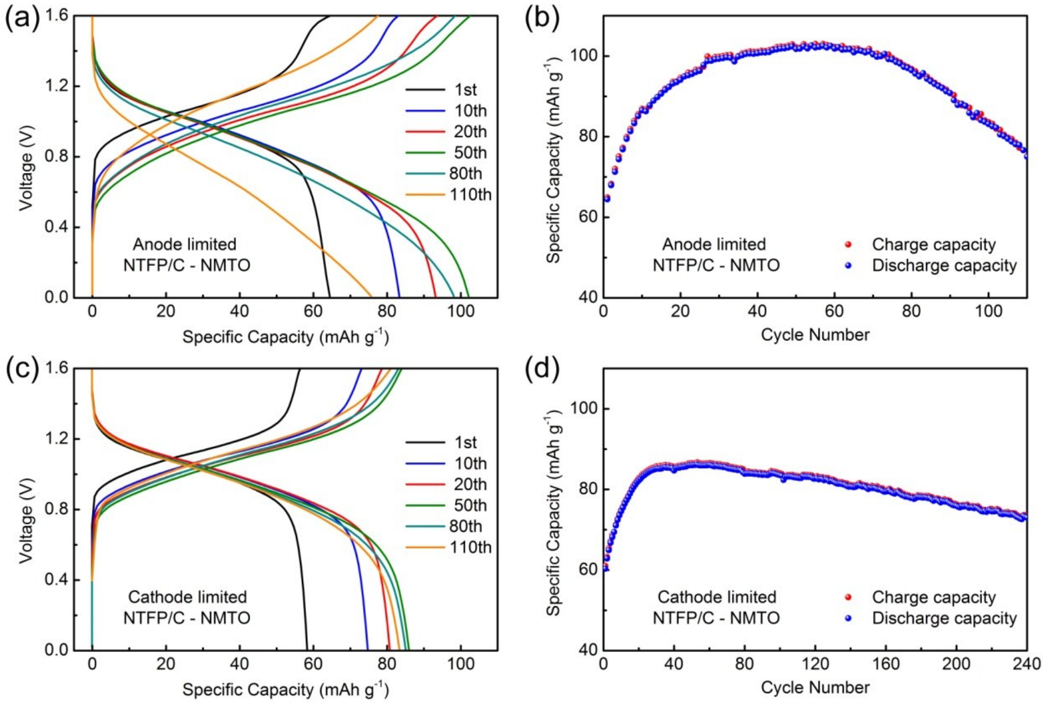


**Fig. S12.** (a, c) Charge-discharge curves and (b, d) cycle performance of the (a, b) Cathode and (c, d) anode limited style $Na_{0.66}Mn_{0.66}Ti_{0.34}O_2$-$Na_{1.5}Ti_{1.5}Fe_{0.5}(PO_4)_3$/C (NMTO-NTFP/C) aqueous full cells at 2 C rate.

For $Na_{0.66}Mn_{0.66}Ti_{0.34}O_2$-$Na_{1.5}Ti_{1.5}Fe_{0.5}(PO_4)_3$/C (NMTO-NTFP/C) aqueous full cell, when it is anode limited, the overcharging of anode will produce a certain degree of hydrogen evolution, leading to the rapid deterioration of the cycle performance of the cell with the accumulation of gas. When it is cathode limited, the specific capacity of the cell is low due to the limited $Na^+$ provided by cathode, and in the subsequent cycle, the material structure of cathode is gradually destroyed due to overcharging, leading to the gradual attenuation of the cell capacity.

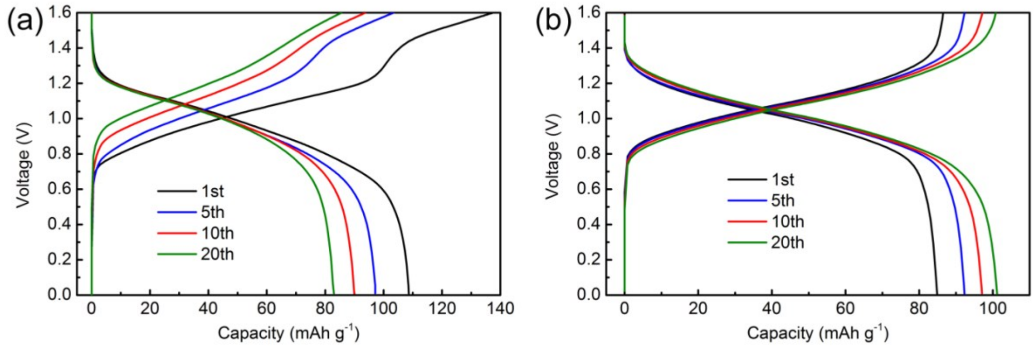


**Fig. S13.** The first 20 cycles Charge-discharge curves of (a) $Na_{0.66}Mn_{0.66}Ti_{0.34}O_2$-$NaTi_2(PO_4)_3$/C (NMTO-NTP/C) and (b) $Na_{0.66}Mn_{0.66}Ti_{0.34}O_2$-$Na_{1.5}Ti_{1.5}Fe_{0.5}(PO_4)_3$/C (NMTO-NTFP/C) aqueous full-cells at 2C rate.

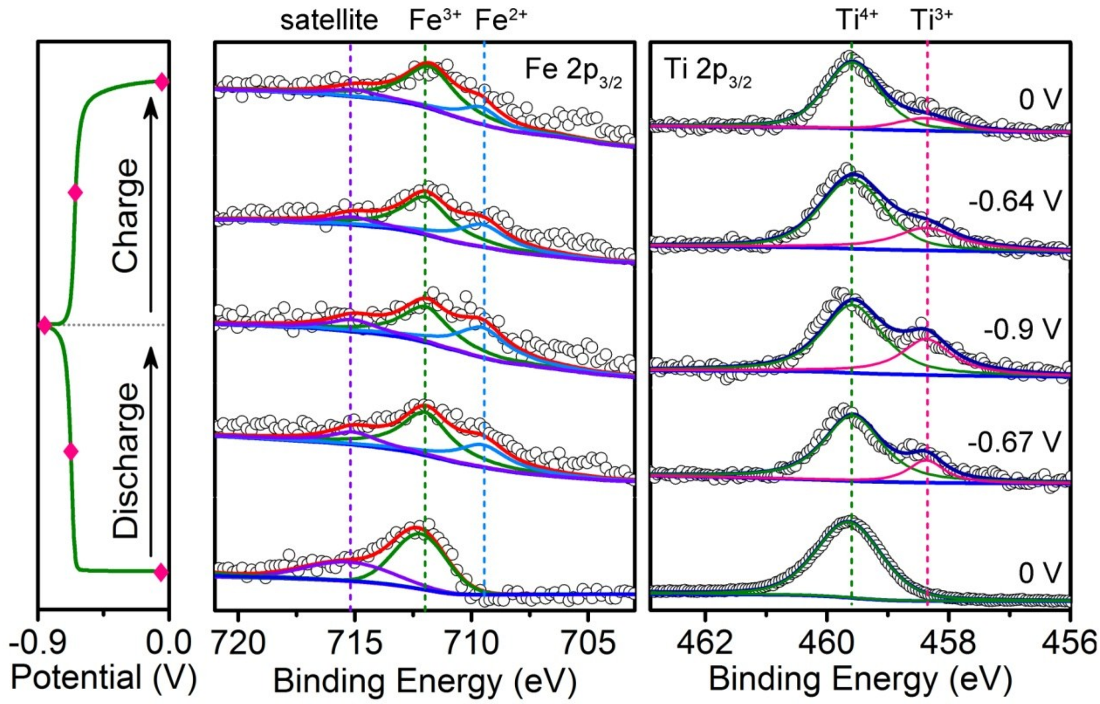


**Fig. S14.** *Ex-situ* XPS spectra of Fe $2p_{3/2}$ and Ti $2p_{3/2}$ for $Na_{1.5}Ti_{1.5}Fe_{0.5}(PO_4)_3$/C (NTFP/C) electrode at various charge-discharge states in the aqueous half cell.

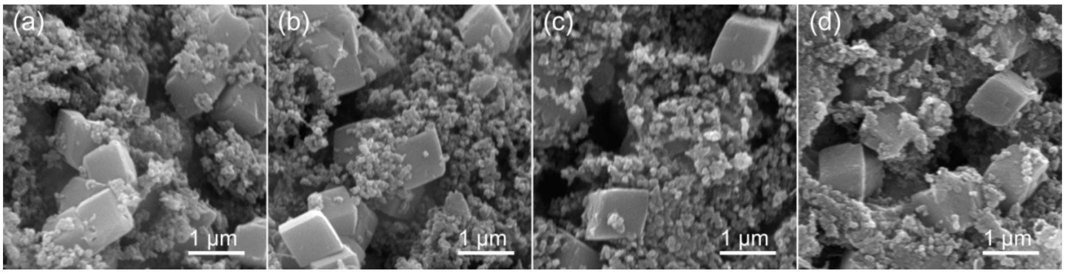


**Fig. S15.** SEM images of $Na_{1.5}Ti_{1.5}Fe_{0.5}(PO_4)_3/C$ (NTFP/C) electrode after charged-discharged (rate: 2 C) in the aqueous full cell for (a) 0 cycles, (b) 10 cycles, (c) 50 cycles, and (d) 100 cycles. The NTFP/C kept its original morphology after long time cycle test.